Scientia Iranica B (2015) 22(3), 865–870

SCIENTIA IRANICA

Sharif University of Technology

Scientia Iranica

Transactions B: Mechanical Engineering

www.scientiairanica.com

Research Note

Fine-tuned double-deck Stewart platform using base excitation with a 6DOF piezo driven hexapod

B. Zahiri[a,1,*] **and M.T. Ahmadian**[b]

a. *School of Mechanical Engineering, Sharif University of Technology, Tehran, Iran.*

b. *Center of Excellence in Design, Robotics and Automation (CEDRA), Sharif University of Technology, Tehran, Iran.*

Received 16 February 2013; received in revised form 27 May 2014; accepted 3 March 2015

KEYWORDS

Parallel mechanism;
Stewart platform;
Stewart workspace;
Particle swarm optimization method;
Piezo actuators;
Double-deck platform;
Error analysis;
Fine tuning mechanism.

Abstract. A parallel mechanism was designed and developed to perform tasks with micro meter accuracy within millimeter-range workspace. The system employs two Stewart platforms while squiggle motors were used in one of the platforms to provide larger workspace, the second platform which uses piezoelectric actuators accurately positions the tool tip in the desired point. Error model for tool tip was developed for the first platform. Considering worst case scenario and using Particle Swarm Optimization algorithm, positioning error of the first platform was evaluated numerically throughout the respective workspace, upon which the design of the fine tuning piezo driven second stage was carried out. Positioning error and workspace of the whole system was evaluated using a single-deck platform with squiggle motors caused 40 micrometers positioning error while application of the fine-tuning piezo-driven Stewart platform reduced the total positioning error to 10 micrometers.

1. Introduction

Micro-positioning techniques have been increasingly used in various fields of engineering such as biomedical applications, semiconductor and microscopy during the past two decades. Due to their numerous merits in terms of stiffness, manipulability, payload and precision, Stewart platforms have been recently used widely for such applications.

When considering application of Stewart platform for the precision positioning, one of the most challenging tradeoffs is the one between the workspace of the mechanism and the accuracy of the endeffector. Larger workspace for the platform calls for actuators with higher stroke range which often provide less resolution. Since the demand of high precision, piezoelectric actuators is used in one of the platforms. Piezo actuators provide nanometer resolution and high stiffness and are quite suitably used in precision positioning platforms. Low stroke range in piezoelectric actuators results in platform with small workspace. To overcome this effect, piezo-driven platform is designed to compensate the position error at the tool tip generated by a Stewart platform which employs squiggle motors as actuators.

Several methodologies (methods) have been used by researchers to drive the error model for Stewart platforms. Li et al. [1] studied the error modeling of parallel mechanisms. They developed an error mapping model that can be used for various configurations of parallel mechanisms. Du et al. [2] studied the error model in a parallel robot. Using Edgeworth series they developed the probability distribution of the mechanism error. Wang et al. [3] presented the first and second order error model for 6 DOF Stewart

1. *Present address: Daniel J. Epstein Department of Industrial and Systems Engineering, 3710 McClintock Ave, RTH 319, Los Angeles, CA, 90089-0063, USA.*

*. *Corresponding author. Tel.: (+1) 213-4773841; E-mail addresses: bzahiri@usc.edu (B. Zahiri); ahmadian@sharif.edu (M.T. Ahmadian)*

platforms. Using sensitivity analysis, they described the contribution of each error component to the total position and orientation error of the mechanism.

This paper suggests error model at the tip of tool mounted on top of Stewart platform. Considering worst case scenario and using Particle Swarm optimization algorithm, positioning error of this platform, which employs squiggle motors as actuators, was evaluated numerically throughout the respective workspace. Error in position, generated by the first platform, was compensated by a high-accuracy piezo-driven Stewart platform and the overall accuracy of the system was evaluated.

2. The pose error model of Stewart platform

The Stewart platform is composed of a movable platform connected to a fixed base through six extendable links, as shown in Figure 1. An error model is developed to identify the positioning error of end-effector.

For this purpose two coordinate systems $\{B\}$ and $\{P\}$ are assigned to the lower (base) and upper (payload) platforms, respectively. The origin of each coordinate system is fixed at the center of each platform, $\{B_c\}$ and $\{P_c\}$. Orientation of the upper coordinate system, $\{P\}$, with respect to the base coordinate system, $\{B\}$, can be defined by a rotation transformation matrix as the following equation:

$$R = R(z,\alpha)R(y,\beta)R(z,\gamma)$$

$$= \begin{bmatrix} C_\beta C_\alpha & S_\gamma S_\beta C_\alpha - C_\gamma S_\alpha & C_\gamma S_\beta C_\alpha + S_\gamma S_\alpha \\ C_\beta S_\alpha & S_\gamma S_\alpha S_\beta + C_\gamma C_\alpha & C_\gamma S_\beta S_\alpha - S_\gamma C_\alpha \\ -S_\beta & S_\gamma C_\beta & C_\gamma C_\beta \end{bmatrix}. \quad (1)$$

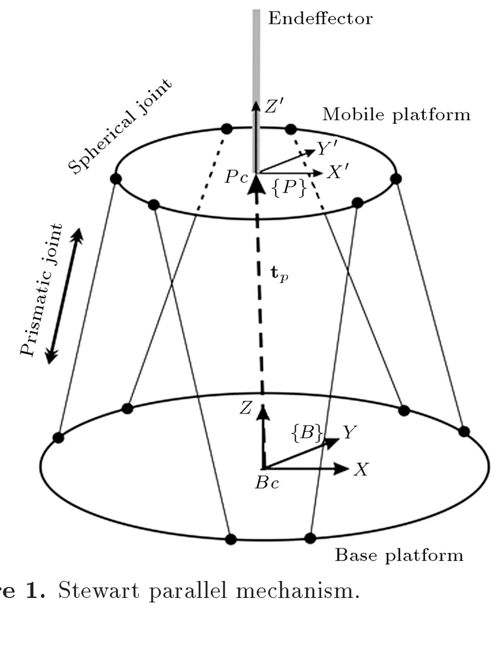

Figure 1. Stewart parallel mechanism.

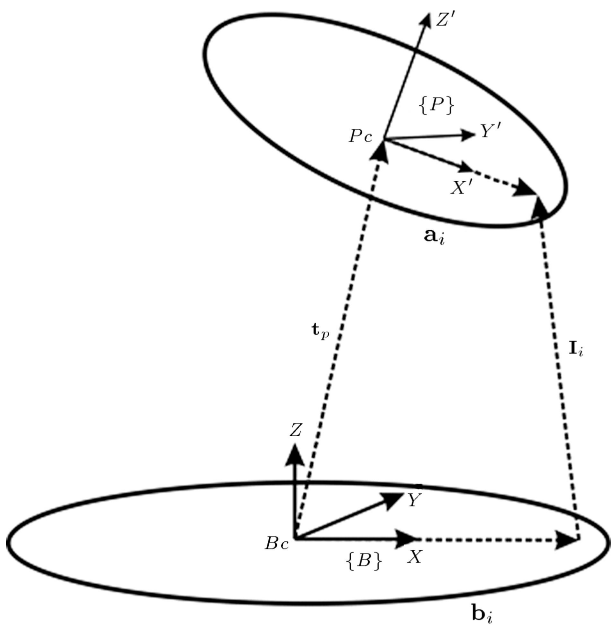

Figure 2. Vector analysis of a single leg.

In Eq. (1), α is the rotation about z axis (Yaw), while β and γ are the rotation angles about the new y and x axes, respectively (Pitch and Roll) [4].

From the vector analysis of a single leg as shown in Figure 2, the following relationship between the position of the upper platform with respect to the base platform, $\mathbf{t}_P$, and the ith leg length, $\mathbf{l}_i(1 = 1, 2, \cdots, 6)$, can be obtained:

$$^B\mathbf{t}_P + {}^B\mathbf{p}_i - {}^B\mathbf{l}_i - {}^B\mathbf{b}_i = {}^B\mathbf{t}_P + R_P.{}^P\mathbf{p}_i - L_i{}^B\mathbf{u}_i - {}^B\mathbf{b}_i = 0. \quad (2)$$

In Eq. (2), $\delta\mathbf{p}_i$ and $\delta\mathbf{b}_i$ are the positions of the ith leg joints on the upper and base platforms; $\mathbf{u}_i$ is the unit vector along the ith leg; and L_i is the corresponding leg length. Using variation principle on both sides of Eq. (2), following equation is derived:

$$\delta\mathbf{t}_P + \delta R.\mathbf{p}_i + R.\delta\mathbf{p}_i - \delta L_i\mathbf{u}_i - L_i\delta\mathbf{u}_i - \delta\mathbf{b}_i = 0. \quad (3)$$

For the rotation matrix R, the following relation can be written [5]:

$$\delta R = \Omega.R = \delta\boldsymbol{\omega} \times R, \quad (4)$$

where Ω is a 3×3 skew symmetric matrix where its nonzero elements represent the angular error $\delta\omega$ of the coordinate systems $\{P\}$; Ω and $\delta\omega$ can be written as [6]:

$$\Omega = \begin{bmatrix} 0 & -\delta\alpha & \delta\beta \\ \delta\alpha & 0 & -\delta\gamma \\ -\delta\beta & \delta\gamma & 0 \end{bmatrix}, \qquad \delta\omega = \begin{bmatrix} \delta\gamma & \delta\beta & \delta\alpha \end{bmatrix}.$$

Hence Eq. (1) can be written as:

$$\delta L_i \mathbf{u}_i + L_i \delta \mathbf{u}_i = \delta \mathbf{t}_P + \delta \boldsymbol{\omega} \times R.\mathbf{p}_i + R.\delta \mathbf{p}_i - \delta \mathbf{b}_i. \tag{5}$$

For the unit vector $\mathbf{u}_i$, $\mathbf{u}_i^T.\mathbf{u}_i = 1$ and $\mathbf{u}_i^T.\delta\mathbf{u}_i = 0$. Multiplying both sides of Eq. (5) by the unit vector $\mathbf{u}_i^T$ and using the two properties for $\mathbf{u}_i$, the following is obtained:

$$\mathbf{u}_i^T.\delta L_i \mathbf{u}_i + \mathbf{u}_i^T.L_i \delta \mathbf{u}_i = \mathbf{u}_i^T.\delta \mathbf{t}_P + \mathbf{u}_i^T.(\delta\omega \times R.\mathbf{p}_i) + \mathbf{u}_i^T.(R.\delta\mathbf{p}_i) - \mathbf{u}_i^T.\delta\mathbf{b}_i$$

$$\Rightarrow \delta L_i = \mathbf{u}_i^T.\delta \mathbf{t}_P + \mathbf{u}_i^T.(\delta\boldsymbol{\omega} \times R.\mathbf{p}_i) + \mathbf{u}_i^T.(R.\delta\mathbf{p}_i) - \mathbf{u}_i^T.\delta\mathbf{b}_i$$

$$\Rightarrow \delta L_i = \begin{bmatrix} \mathbf{u}_i^T & (R.\mathbf{p}_i \times \mathbf{u}_i)^T \end{bmatrix} \begin{bmatrix} \delta \mathbf{t}_P \\ \delta \boldsymbol{\omega} \end{bmatrix} + \begin{bmatrix} \mathbf{u}_i^T R & -\mathbf{u}_i^T \end{bmatrix} \begin{bmatrix} \delta \mathbf{p}_i \\ \delta \mathbf{b}_i \end{bmatrix}. \tag{6}$$

The joint error vector of the top and bottom platforms, $\delta\mathbf{p}_i$ and $\delta\mathbf{b}_i$ can be described in the respective coordinate systems as [7]:

$$\delta\mathbf{p}_i = (\delta p_{ix}, \delta p_{iy}, \delta p_{iz}), \qquad \delta\mathbf{b}_i = (\delta b_{ix}, \delta b_{iy}, \delta b_{iz}).$$

Eq. (6) can be simplified as the following equation [2]:

$$\delta \mathbf{l} = J_P.\begin{bmatrix} \delta \mathbf{t}_P \\ \delta \boldsymbol{\omega} \end{bmatrix} + J_C.\begin{bmatrix} \delta \mathbf{p}_i \\ \delta \mathbf{b}_i \end{bmatrix}, \tag{7}$$

where:

$$J_P = \begin{bmatrix} \mathbf{u}_1^T & (R.\mathbf{p}_1 \times \mathbf{u}_1)^T \\ \vdots & \vdots \\ \vdots & \vdots \\ \mathbf{u}_6^T & (R.\mathbf{p}_6 \times \mathbf{u}_6)^T \end{bmatrix} \in R^{6\times 6},$$

$$J_C = \begin{bmatrix} \mathbf{u}_1^T R & -\mathbf{u}_1^T & \cdots & \cdots & 0 & 0 \\ \vdots & \vdots & \ddots & \ddots & \vdots & \vdots \\ \vdots & \vdots & \ddots & \ddots & \vdots & \vdots \\ 0 & 0 & \cdots & \cdots & \mathbf{u}_6^T R & -\mathbf{u}_6^T \end{bmatrix} \in R^{6\times 36}.$$

From Eq. (7), pose error of the mechanism is obtained as:

$$\begin{bmatrix} \delta \mathbf{t}_P \\ \delta \boldsymbol{\omega} \end{bmatrix} = J_P^{-1}.\left(\delta \mathbf{l} - J_C.\begin{bmatrix} \delta \mathbf{p}_i \\ \delta \mathbf{b}_i \end{bmatrix}\right). \tag{8}$$

Using triangle inequality one may write:

$$\begin{bmatrix} \delta \mathbf{t}_P \\ \delta \boldsymbol{\omega} \end{bmatrix} \leq J_P^{-1}.\delta \mathbf{l} + J_P^{-1}.J_C.\begin{bmatrix} \delta \mathbf{p}_i \\ \delta \mathbf{b}_i \end{bmatrix}. \tag{9}$$

For the tip of a tool mounted on the top of Stewart platform, the position error is defined as the following equation:

$$\delta \mathbf{t}_{\mathrm{Tool}} \leq \delta \mathbf{t}_P + \mathrm{Rot}(\delta\gamma, \delta\beta, 0).\begin{bmatrix} 0 \\ 0 \\ h \end{bmatrix}, \tag{10}$$

where h is the distance of the tool tip to the plane of the upper joints and:

$$\mathrm{Rot}(\delta\gamma, \delta\beta, 0) = R(z, 0)R(y, \delta\beta)R(x, \delta\gamma),$$

where $\delta\gamma$ and $\delta\beta$ originate from $\delta\omega$ which is the orientation error at the center of top platform.

3. Results and discussion

For simplicity, we refer to the first stage Stewart platform with squiggle motors as SP1, and the fine tuning piezo-driven Stewart platform as SP2.

Eqs. (9) and (10) indicate that error vectors, in the left side of these equations, vary for different locations of workspace. For a given position and orientation in the workspace of SP1, error vector is a function of 42 variables ($\delta\mathbf{l}, \delta\mathbf{p}_i, \delta\mathbf{b}_i \; i = 1 \sim 6$), each having an upper and lower bound according to actuator resolution and manufacturing tolerances. In order to find the maximum position and orientation error and employing the worst case scenario method, 260 locations in the region defined by $\{X, Y, Z > 0,\ \gamma = \beta = \alpha = 0\}$ and within the workspace of SP1 are selected, and for each point, Particle Swarm Optimization algorithm is used to find maximum error for each degree of freedom. Squiggle motors were used in SP1 as actuators [8]. These actuators provide resolution about 1 μm, also the manufacturing and assembling tolerances used were less than 10 μm.

Using Eq. (9), the maximum possible error in the center of the top platform for each degree of freedom ($\delta X, \delta Y, \delta Z, \delta\gamma, \delta\beta, \delta\alpha$) is depicted in Figures 3-8 throughout the workspace of SP1 and in the region $\{X, Y, Z > 0,\ \gamma = \beta = \alpha = 0\}$ using Particle Swarm Optimization algorithm and considering the worst case scenario.

Position error distribution at the tip of a tool mounted on top of SP1 is illustrated in Figures 9-12. The distance; h, for the tool used, was 2 cm.

Design of SP2 was based on the error distribution of tool tip generated by SP1. From the error distribution shown in Figure 12, piezo actuators in SP2 should provide enough strokes so that the workspace created by SP2 at tool tip can completely cover this error criterion throughout the workspace of SP1. Figure 13 shows the workspace of the fine tuning platform with 3 cm piezo actuators, which is the minimum required length for piezo actuators. Workspace shown in this figure is created by second Stewart platform at tool tip

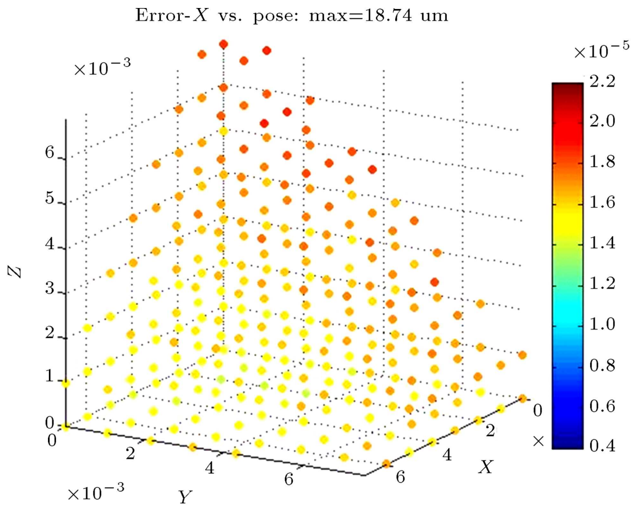

Figure 3. The variation of position error in x-direction in 1/8 of workspace.

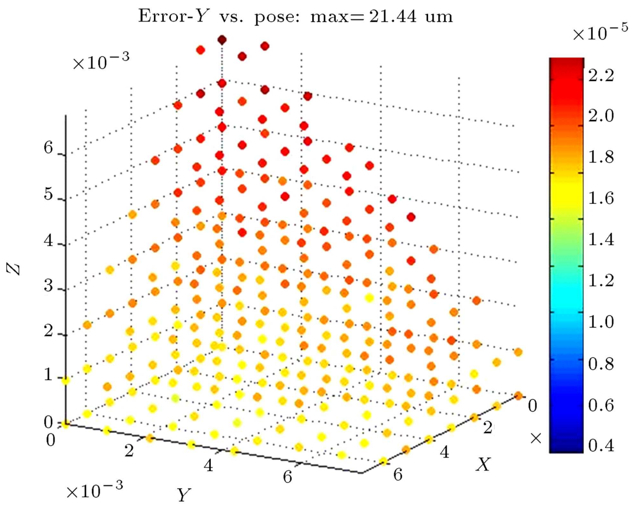

Figure 4. The variation of position error in y-direction in 1/8 of workspace.

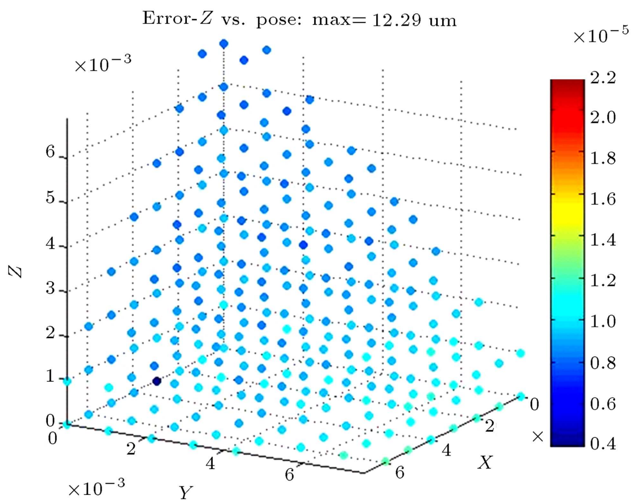

Figure 5. The variation of position error in z-direction in 1/8 of workspace.

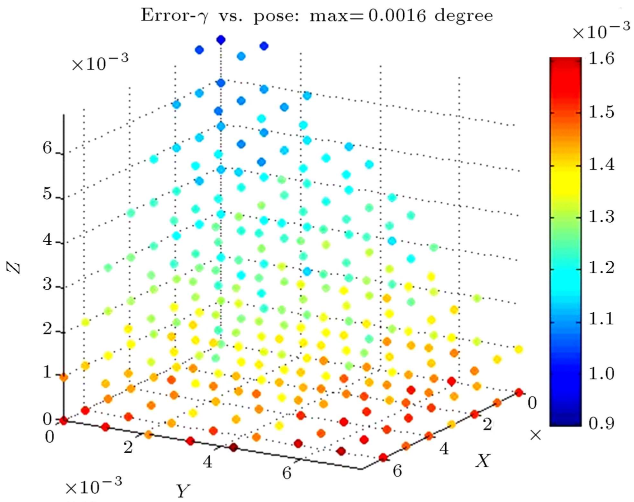

Figure 6. The variation of orientation error for the orientation angle γ in 1/8 of workspace.

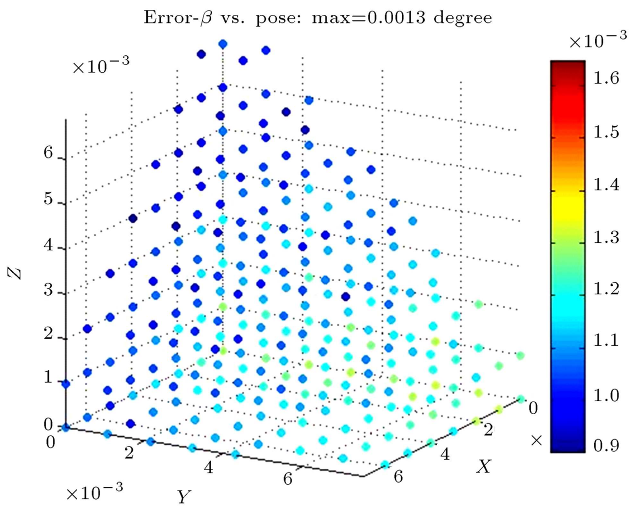

Figure 7. The variation of orientation error for the orientation angle β in 1/8 of workspace.

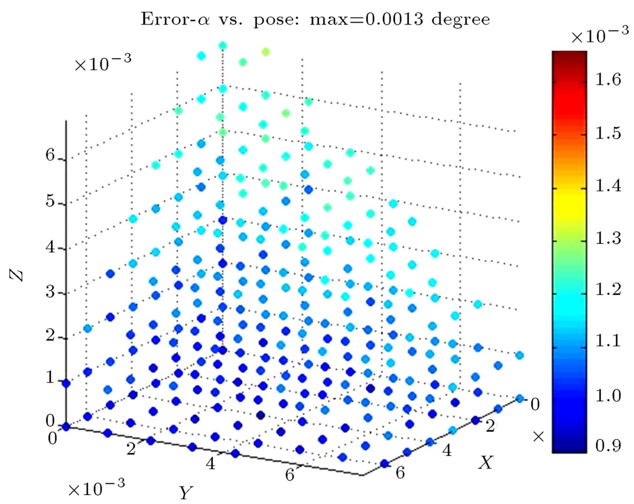

Figure 8. The variation of orientation error for the orientation angle α in 1/8 of workspace.

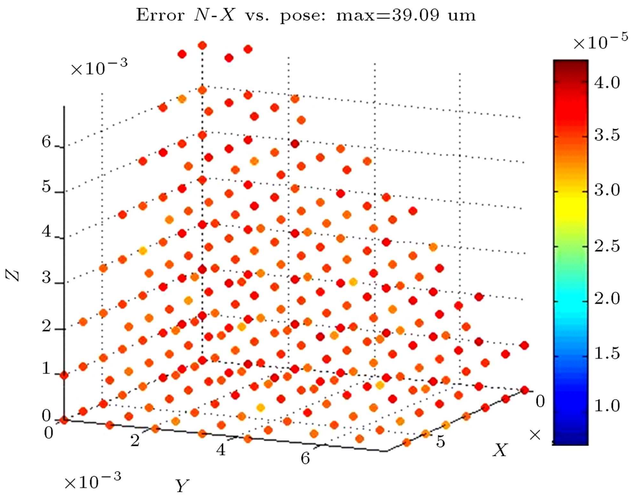

Figure 9. The variation of position error in x-direction at the top of endeffector in 1/8 of workspace.

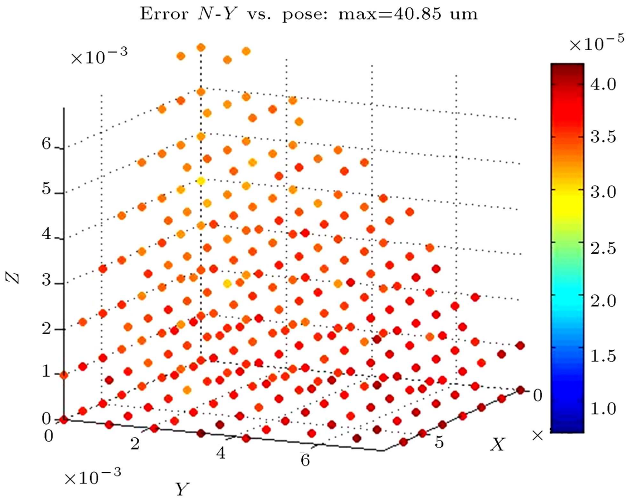

Figure 10. The variation of position error in y-direction at the top of endeffector in 1/8 of workspace.

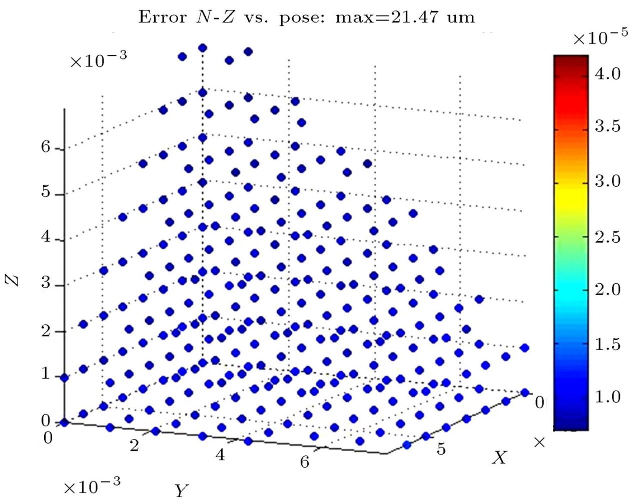

Figure 11. The variation of position error in z-direction at the top of endeffector in 1/8 of workspace.

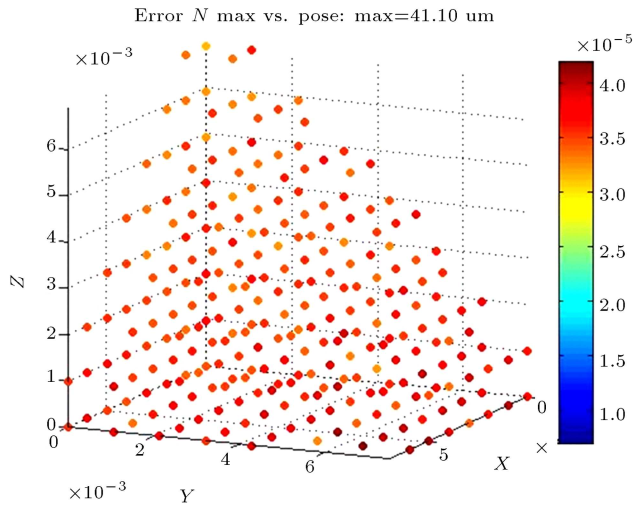

Figure 12. The variation of maximum position error in x, y or z direction at the top of endeffector in 1/8 of workspace.

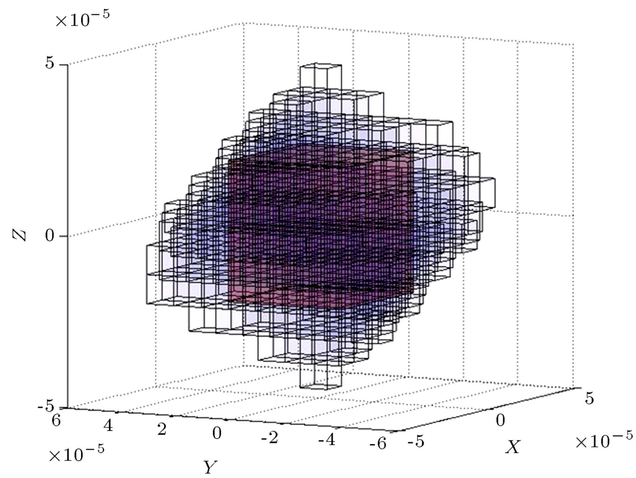

Figure 13. Workspace of fine tuning platform with 3 cm piezo actuators. The middle big cube is the position error region of SP1.

and totally covers the error region generated by SP1, which is shown by the bigger cube inside. Hysteresis effects for piezo actuators can then be modeled by dynamic Preisach model, and by designing controller for the piezo actuators and using backlash-free flexural joints, each leg in the SP2 would provide nanometer resolution [9]. The overall error in position for the two layer mechanism is shown in Figure 14 which is about 8.8 μm. Error compensation methods can be used to reduce the assembling errors of SP2 and further increase the accuracy of the fine tuning stage to sub-micron level.

4. Conclusion

In this study, fine tuning of a Stewart platform was performed using base adjustment with a high accuracy

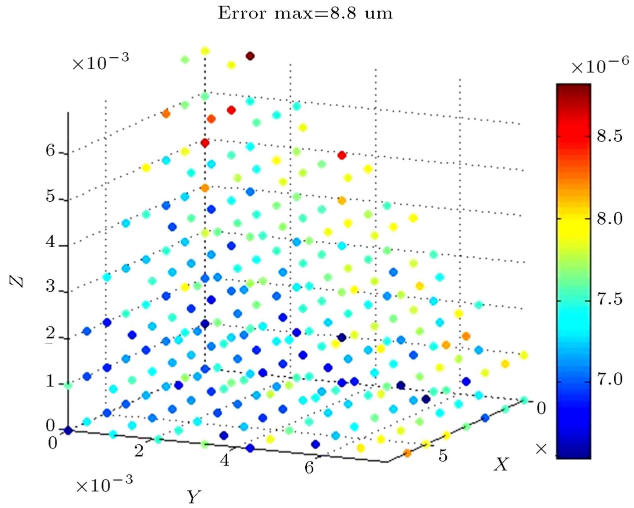

Figure 14. The variation of maximum position error for the fine tuning stage in x, y or z direction at the tip of endeffector in 1/8 of workspace of SP1.

piezo-driven hexapod while the whole structure acts like a double-deck Stewart platform. Error model for a tool mounted on top of the first stage was developed and by using Particle Swarm Optimization algorithm and considering the worst case scenario, the maximum error for each degree of freedom was evaluated numerically throughout the corresponding workspace. Upon this error distribution, the design of the fine tuning second stage was carried out. Using double-deck Stewart platform, positioning within 10 micrometers of the target was achieved. By using compensation techniques, it is possible to reduce the manufacturing and assembling errors and further increase the accuracy of the double-deck platform to sub-micron level.

References

1. Li, T. and Ye, P. "The measurement of kinematic accuracy for various configurations of parallel manipulators", *IEEE International Conference*, **2**, pp. 1122-1129 (2003).
2. Du, Y., Xie, P. and Liu, B. "Error analysis in parallel robot using Edgeworth series and information entropy", *International Conference on Computer Design and Applications*, **2**, pp. 350-354 (2010).
3. Wang, S.-M. and Ehmann, K.F. "Error model and accuracy analysis of a six-DOF Stewart platform", *Journal of Manufacturing Science and Engineering*, **124**(2), pp. 286-295 (2002).
4. Ting, Y., Jar, H.-C. and Li, C.-C. "Measurement and calibration for Stewart micromanipulation system", *Precision Engineering*, **31**(3), pp. 226-233 (2007).
5. Ting, Y., Jar, H. and Li, C. "Error compensation and feed-forward controller design for a 6-DOF micro-positioning platform", *Intelligent Robots and Systems Conference*, pp. 942-947 (2005).
6. Schilling, R.J., *Fundamentals of Robotics: Analysis & Control*, 1st Edn., Prentice Hall (1990).
7. Tsai, L.W., *Robot Analysis: The Mechanics of Serial and Parallel Manipulator*, pp. 142-151, John Wiley & Sons, New York, USA (1999).
8. Newscale Technologies, Inc., http://www.newscaletech.com/
9. Awtar, S. and Parmar, G. "Design of a large range *XY* nano-positioning system", *Proceedings of the ASME Design Engineering Technical Conferences*, pp. 387-399 (2010).

Biographies

Behnam Zahiri received his MSc degree in Mechanical Engineering in 2010 from Sharif University of Technology, Tehran, Iran. He is now a PhD candidate of Industrial and Systems Engineering at University of Southern California and a research assistant at the Center for Rapid Automated Fabrication Technologies (CRAFT) at USC. His research is currently focused on: robotics, 3D printing and contour crafting.

Mohamad Taghi Ahmadian received his BS and MS degrees in Physics, in 1972 from Shiraz University, Shiraz, Iran and completed the requirements for BS and MS degree in Mechanical Engineering, 1980, in University of Kansas in Lawrence. At the same time he completed his PhD in Physics, and PhD in Mechanical Engineering in 1981 and 1986, respectively, in University of Kansas. His research interests are micro and nano mechanics as well as Bioengineering.